Simple optimized Brenner potential for thermodynamic properties of diamond

F. Liu [a] , Q.H. Tang [a] , B.S. Shang [a] & T.C. Wang [a]

[a] State Key Laboratory of Nonlinear Mechanics, Institute of
Mechanics, Chinese Academy of Sciences, Beijing, China
Version of record first published: 31 Oct 2011.

PLEASE SCROLL DOWN FOR ARTICLE

Taylor & Francis
Taylor & Francis Group

Simple optimized Brenner potential for thermodynamic properties of diamond

F. Liu, Q.H. Tang, B.S. Shang and T.C. Wang*

*State Key Laboratory of Nonlinear Mechanics, Institute of Mechanics,
Chinese Academy of Sciences, Beijing, China*

We have examined the commonly used Brenner potentials in the context of the thermodynamic properties of diamond. A simple optimized Brenner potential is proposed that provides very good predictions of the thermodynamic properties of diamond. It is shown that, compared to the experimental data, the lattice wave theory of molecular dynamics (LWT) with this optimized Brenner potential can accurately predict the temperature dependence of specific heat, lattice constant, Grüneisen parameters and coefficient of thermal expansion (CTE) of diamond.

Keywords: lattice wave theory; thermodynamic properties; optimized Brenner potential; diamond; finite temperature

1. Introduction

There has been a surge of interest in efforts to account for the effects of finite temperature in multiscale methods and atomistic-based continuum theories. To achieve this goal, several models, such as local harmonic model (LHM), local quasiharmonic model (LQHM), quasiharmonic model in real space (QHM) and quasiharmonic model in the reciprocal space or the k-space (QHMK), can be used.

The quasicontinuum (QC) method proposed by Tadmor et al. [1,2] is a mixed continuum and atomistic approach, which significantly reduces the total number of degrees of freedom and deals with only the mechanical response of crystalline materials at zero temperature. To accurately predict the mechanical behavior of nanosystems, it is necessary to take into account the effect of finite temperature. With LHM, the QC approach has been extended to deal with finite-temperature solid systems [3–5]. In [3,4], a QC Monte Carlo (QCMC) method and a QC free energy minimization (QCFEM) method were proposed to study equilibrium properties of defects at finite temperature. Arroyo and Belytschko [6], Zhang et al. [7–10] and Jiang et al. [11] have proposed nanoscale continuum theories for carbon nanotubes based on interatomic potentials for carbon. Based on the local harmonic approximation [12], Jiang et al. [13] established a finite-temperature continuum theory directly from the interatomic potential. The interatomic potential is incorporated into the continuum analysis via the constitutive model and the effect of finite temperature is also taken into

*Corresponding author. Email: tcwang@imech.ac.cn

account. Such an approach has the advantage of accounting for the finite temperature effect but avoiding the use of molecular dynamics or Monte Carlo simulation, which are computationally intensive and not suitable for large-scale problems. Zhao et al. [14] studied the bulk thermodynamic properties of crystalline silicon using three quasiharmonic models with the Tersoff interatomic potential: QHM, QHMK and LQHM. QHMK was recommended for its low computational cost and high accuracy.

With the development of these multiscale methods and atomistic-based continuum theories at finite temperature, multi-body potentials are being used to study the thermodynamic and mechanic properties of covalently bonded systems, and there is no doubt that an accurate interatomic potential is the crucial ingredient for obtaining meaningful properties [15]. A successful method for treating covalent bonding interactions in computation is the Tersoff-type potential [16,17]. The Tersoff model, in comparison with traditional molecular mechanics force fields [18–25], allows for the formation and dissociation of covalent chemical bonds during a simulation. Multi-body terms reflecting the local coordination environment of each atom are used to modify the strength of more conventional pairwise terms [26]. One particularly successful example of Tersoff potential is the Brenner potential, which is developed by Brenner [27–29]. This model has re-parameterized the Tersoff potential and added nonlocal terms to properly account for the bond modification induced by a change of bonding of neighboring atoms [30]. However, since the parameters of the Tersoff and Brenner potentials are fitted by a little experimental data, such as binding energy, lattice constant, etc, neither of them can accurately predict the thermodynamic properties of carbon based structures.

In this paper, the lattice wave theory of molecular dynamics [31] (LWT) is used to study the thermodynamic properties of diamond. A simple optimized Brenner potential with optimized parameter sets is proposed. The present calculation results for thermodynamic properties of diamond have found very good agreements with experimental data, which can illustrate the validity of this theory and also the optimized Brenner potential.

This paper is divided into seven sections. First, we will review the Brenner potential in Section 2. Then the LWT will be briefly introduced in Section 3. In Section 4, LWT is specified for diamond, and parameter optimization for Brenner potential will be given in Section 5. In Section 6 the calculation results for the thermodynamics properties of diamond, including specific heat, the coefficient of thermal expansion (CTE), lattice constant and Grüneisen parameters, are presented and compared with experimental data.

2. Brenner potential

The total potential energy, U_{tot}, of a system of N atoms is given by

$$U_{\text{tot}} = \frac{1}{2} \sum_i \sum_{j \neq i} V_{ij}, \tag{1}$$

where V_{ij} is the interatomic potential energy that is stored in the bond between atoms i and j. In Brenner potential [27] for carbon, V_{ij} takes the form

$$V_{ij} = V_R(r_{ij}) - \bar{B}_{ij} V_A(r_{ij}). \tag{2}$$

where r_{ij} is the bond length or the distance between atoms i and j, $V_R(r)$ and $V_A(r)$ are pair-additive repulsive and attractive interactions, respectively,

$$V_{ij} = V_R(r_{ij}) - \bar{B}_{ij} V_A(r_{ij}) \tag{3}$$

and

$$V_A(r) = \frac{D^{(e)} S}{S - 1} e^{-\sqrt{2/S}\beta[r - R^{(e)}]} f_C(r). \tag{4}$$

f_C is merely a smooth cut-off function having the piecewise form

$$f_C(r) = \begin{cases} 1 & r < R^{(1)} \\ \frac{1}{2}\left\{1 + \cos\left[\frac{\pi(r - R^{(1)})}{R^{(2)} - R^{(1)}}\right]\right\} & R^{(1)} < r < R^{(2)} \\ 0 & r > R^{(2)} \end{cases}. \tag{5}$$

The factor $\bar{B}_{ij}$ in Equation (2) can be expressed as

$$\bar{B}_{ij} = \frac{1}{2}(B_{ij} + B_{ji}) \quad B_{ij} = \left[1 + \sum_{k(\neq i,j)} G(\theta_{ijk}) f_c(r_{ik})\right]^{-\delta_t}; \tag{6}$$

where $\cos\theta_{ijk} = (r_{ij}^2 + r_{ik}^2 - r_{jk}^2)/(2r_{ij}r_{ik})$ is the angle between carbon bonds $i - j$ and $i - k$; the function G takes the form

$$G(\theta) = a_0\left[1 + \frac{c_0^2}{d_0^2} - \frac{c_0^2}{d_0^2 + (1 + \cos\theta)^2}\right] \tag{7}$$

where $a_0 = 0.00020813$, $c_0 = 330$, $d_0 = 3.5$, and other parameters mentioned above can be found in [27] ($D^{(e)} = 6.000\,\text{eV}$, $S = 1.22$, $\beta = 21\,\text{nm}^{-1}$, $R^{(e)} = 0.1390\,\text{nm}$, $\delta^t = 0.5$, $R^{(1)} = 0.17\,\text{nm}$, $R^{(2)} = 0.2\,\text{nm}$).

The state of equilibrium is determined by minimizing the total potential energy in Equation (1) with respect to atom positions.

$$\frac{\partial U_{\text{tot}}}{\partial \mathbf{r}_i} = 0. \tag{8}$$

Using the chain rule, we have

$$\mathbf{f}_i = -\frac{\partial U_{\text{tot}}}{\partial \mathbf{r}_i} = -\sum_{j \in \Omega_i} \frac{\partial U_{\text{tot}}}{\partial r_{ij}} \frac{\partial r_{ij}}{\partial \mathbf{r}_i} = \sum_{j \in \Omega_i} \frac{\partial U_{\text{tot}}}{\partial r_{ij}} \mathbf{e}_{ij}$$

$$\mathbf{e}_{ij} = \frac{\mathbf{r}_{ij}}{r_{ij}}, \quad i = 1, \ldots, N \tag{9}$$

where Ω_i represents the set of all atoms interact with the i atom, and N is the total atomic number.

Letting $\mathbf{f}_{ij} = \frac{\partial U_{\text{tot}}}{\partial r_{ij}} \mathbf{e}_{ij} = f_{ij} \mathbf{e}_{ij}\, f_{ij} = \frac{\partial U_{\text{tot}}}{\partial r_{ij}}$ we have

$$\mathbf{f}_i = \sum_{j \in \Omega_i} \mathbf{f}_{ij} = 0 \tag{10}$$

where $\mathbf{f}_{ij}$ can be considered the bond force between atoms i and j.

3. Lattice wave theory of molecular dynamics

As discussed by Tang et al. [14,32], the size of the force constant matrix in the quasi-harmonic (QHM) approach is $3N \times 3N$, while the local quasi-harmonic (LQHM) approach reduces the size of the force constant matrix to 3×3 by neglecting all terms in the QHM model that couple vibrations of different atoms. An alternative approach is the QHMK approach, which preserves the coupling of the vibrations of different atoms but significantly reduces the size of the force constant matrix.

In the QHMK approach and the LWT [31], the key idea is that the size of the force constant matrix can be reduced based on the fact that the vibration of the atoms in a Bravais lattice has the same magnitude and direction and only differs in phase [33]. However, instead of the Hamiltonian being expressed in the k-space to find the dynamical matrix, in LWT approach the dynamical matrix can be obtained directly by the dynamic equation of the atom surround its equilibrium position.

Following Tang and Wang [31], the dynamic equation of the atom k can be written as

$$m_k \ddot{\mathbf{u}}_k = \sum_{j \in \Omega_k} \mathbf{K}_{kj} \bullet (\mathbf{u}_j - \mathbf{u}_k) \quad \text{where } \mathbf{K}_{kj} = \frac{f(r_{kj})}{r_{kj}} \mathbf{I} + \left(f'(r_{kj}) - \frac{f(r_{kj})}{r_{kj}}\right)\mathbf{e}_{kj} \otimes \mathbf{e}_{kj} \quad (11)$$

where Ω_k represents the set of atoms which interact with the k atom, m_k is the mass of atom k, $\mathbf{u}_j$ is the displacement of atom j due to thermal vibration, $\mathbf{I}$ is the second-order unit tensor, and $\otimes$ is the tensor multiplication operator; r_{kj} is the radius between the k atom and the j atom, and the direction is from the k atom to the j atom. $\mathbf{e}_{kj}$ is the unit vector.

According to the dynamic theory of crystal lattices [34], the solution of Equation (11) can be expressed as

$$\mathbf{u}_j = \mathbf{A}_j e^{i(\omega t - \mathbf{r}_j \bullet \mathbf{q})}. \quad (12)$$

For a crystal with dimensions $N_1 \mathbf{a}_1$, $N_2 \mathbf{a}_2$, and $N_3 \mathbf{a}_3$ ($\mathbf{a}_1$, $\mathbf{a}_2$ and $\mathbf{a}_3$ are the three basis vectors) and the Born–von Karman boundary condition [35], the allowed values of $\mathbf{q}$ are given by

$$\mathbf{q} = \frac{k_1}{N_1} \mathbf{b}_1 + \frac{k_2}{N_2} \mathbf{b}_2 + \frac{k_3}{N_3} \mathbf{b}_3, \quad k_1 = 1, \ldots, N_1, \quad k_2 = 1, \ldots, N_2, \quad k_3 = 1, \ldots, N_3$$

$$(13)$$

where $\mathbf{b}_1$, $\mathbf{b}_2$ and $\mathbf{b}_3$ are the three basis vectors of the reciprocal lattice.

Substituting Equation (12) into Equation (11), we have

$$m_k \mathbf{A}_k \omega^2 = \sum_{j \in \Omega_k} \mathbf{K}_{kj} \bullet \left(\mathbf{A}_j e^{i \mathbf{r}_{jk} \bullet \mathbf{q}} - \mathbf{A}_k\right) \quad k = 1, \ldots, N \quad (14)$$

where N is the total atomic number and

$$\mathbf{K}_{kj} = \alpha_{kj} \mathbf{I} + \gamma_{kj} \mathbf{e}_{kj} \otimes \mathbf{e}_{kj}$$

$$\alpha_{kj} = \frac{f_{kj}}{r_{kj}}, \quad \beta_{kj} = \frac{\partial f_{kj}}{\partial r_{kj}}, \quad \gamma_{kj} = \beta_{kj} - \alpha_{kj} \quad (15)$$

Equation (14) provides the dynamical matrix of the three-dimensional (3D) crystal.

4. Calculation results for diamond

4.1. *Dynamic equation of diamond*

The diamond lattice consists of two interpenetrating fcc Bravais lattices, displaced along the body diagonal of the cubic cell by one quarter the length of the diagonal.

With the lattice constant of diamond equal to 0.3567 nm, the distance of the first and second nearest neighbors can be calculated as

$$r = \frac{\sqrt{3}}{4} a_0 = \frac{\sqrt{3}}{4} \times 0.3567\,\text{nm} \approx 0.1544\,\text{nm} < 0.17\,\text{nm},$$

$$r' = \frac{\sqrt{2}}{2} a_0 = \frac{\sqrt{2}}{2} \times 0.3567\,\text{nm} \approx 0.2522\,\text{nm} > 0.2\,\text{nm}.$$

For the unit cell of diamond shown in Figure 1, it is obvious from the difference of their geometrical surroundings that carbon atoms in diamond can be classified into two types A and B. Since cut-off function is

$$f_C(r) = \begin{cases} 1 & r < 0.17 \\ \dfrac{1}{2}\left\{1 + \cos\left[\dfrac{\pi(r - 0.17)}{0.2 - 0.17}\right]\right\} & 0.17 < r < 0.2 \\ 0 & r > 0.2 \end{cases},$$
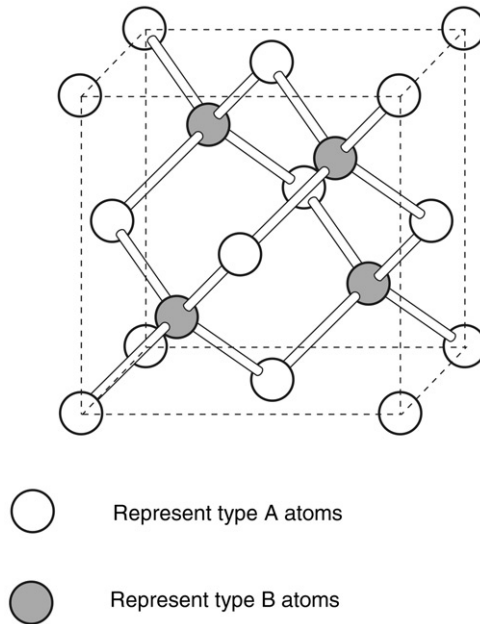

Figure 1. A unit cell of diamond; there are two types of atoms with different geometrical surroundings, and here we use different colors to distinguish these two types of atoms.

one carbon atom interacts with four nearest neighbors, i.e. one type A carbon interacts with four type B carbons, and vice versa.

The dynamic equations therefore can be expressed by

$$m\ddot{\mathbf{u}}_{A_i} = \sum_{j=1}^{4} \mathbf{K}(r_{A_i}B_j) \bullet (\mathbf{u}_{B_j} - \mathbf{u}_{A_i})$$

$$m\ddot{\mathbf{u}}_{B_i} = \sum_{j=1}^{4} \mathbf{K}(r_{B_i}A_j) \bullet (\mathbf{u}_{A_j} - \mathbf{u}_{B_i})$$

(16)

where A and B represent the type of the atom, and i and j are serial numbers of the atom.

The solutions of lattice wave are given by

$$\begin{cases} \mathbf{u}_{A_i} = \mathbf{A}e^{i[\omega t - \mathbf{r}_{A_i} \bullet \mathbf{q}]} \\ \mathbf{u}_{B_i} = \mathbf{B}e^{i[\omega t - \mathbf{r}_{B_i} \bullet \mathbf{q}]} \end{cases}$$

(17)

4.2. *Characteristic equation*

From the diamond lattice shown in Figure 2, the geometrical relation can be written as

$$\mathbf{r}_{A_0} - \mathbf{r}_{B_0} = \frac{a_0}{4}(1, -1, -1);$$

$$\mathbf{r}_{A_0} - \mathbf{r}_{B1} = \frac{a_0}{4}(1, -1, -1); \quad \mathbf{r}_{A_0} - \mathbf{r}_{B2} = \frac{a_0}{4}(-1, 1, -1);$$

$$\mathbf{r}_{A_0} - \mathbf{r}_{B3} = \frac{a_0}{4}(1, 1, 1); \quad \mathbf{r}_{A_0} - \mathbf{r}_{B4} = \frac{a_0}{4}(-1, -1, 1);$$

$$\mathbf{r}_{B_0} - \mathbf{r}_{A1} = \frac{a_0}{4}(-1, 1, 1); \quad \mathbf{r}_{B_0} - \mathbf{r}_{A2} = \frac{a_0}{4}(1, -1, 1);$$

$$\mathbf{r}_{B_0} - \mathbf{r}_{A3} = \frac{a_0}{4}(-1, -1, -1); \quad \mathbf{r}_{B_0} - \mathbf{r}_{A4} = \frac{a_0}{4}(1, 1, -1);$$

(18)

where a_0 is the lattice constant.

Substituting Equation (17) into Equation (16), and taking account for the geometrical relation, we have (for non-deformed or uniform expanding lattice, $\alpha_{ij} = \alpha$ and $\gamma_{ij} = \beta - \alpha$)

$$\begin{pmatrix} 4\alpha + \frac{4}{3}\gamma & 0 & 0 & \left(\alpha + \frac{\gamma}{3}\right)p & \frac{\gamma}{3}p_1 & \frac{\gamma}{3}p_2 \\ 0 & 4\alpha + \frac{4}{3}\gamma & 0 & \frac{\gamma}{3}p_1 & \left(\alpha + \frac{\gamma}{3}\right)p & \frac{\gamma}{3}p_3 \\ 0 & 0 & 4\alpha + \frac{4}{3}\gamma & \frac{\gamma}{3}p_2 & \frac{\gamma}{3}p_3 & \left(\alpha + \frac{\gamma}{3}\right)p \\ \left(\alpha + \frac{\gamma}{3}\right)q & \frac{\gamma}{3}q_1 & \frac{\gamma}{3}q_2 & 4\alpha + \frac{4}{3}\gamma & 0 & 0 \\ \frac{\gamma}{3}q_1 & \left(\alpha + \frac{\gamma}{3}\right)q & \frac{\gamma}{3}q_3 & 0 & 4\alpha + \frac{4}{3}\gamma & 0 \\ \frac{\gamma}{3}q_2 & \frac{\gamma}{3}q_3 & \left(\alpha + \frac{\gamma}{3}\right)q & 0 & 0 & 4\alpha + \frac{4}{3}\gamma \end{pmatrix} \begin{pmatrix} A_x \\ A_y \\ A_z \\ B_x \\ B_y \\ B_z \end{pmatrix} = m\omega^2 \begin{pmatrix} A_x \\ A_y \\ A_z \\ B_x \\ B_y \\ B_z \end{pmatrix}$$
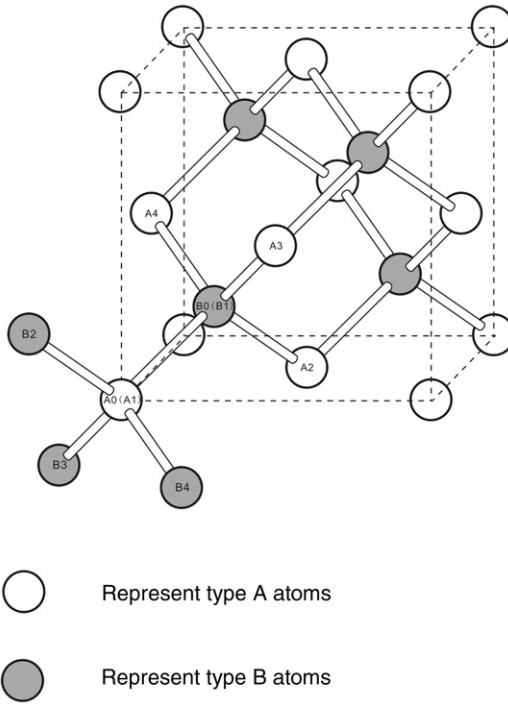
(19)

Figure 2. Several atoms which we are interested in are labeled by their type first and serial number second.

where

$$p = -\left(e^{i[\frac{a_0}{4}(q_x-q_y-q_z)]} + e^{i[\frac{a_0}{4}(-q_x-q_y+q_z)]} + e^{i[\frac{a_0}{4}(q_x+q_y+q_z)]} + e^{i[\frac{a_0}{4}(-q_x+q_y-q_z)]} \right)$$

$$p_1 = -\left(-e^{i[\frac{a_0}{4}(q_x-q_y-q_z)]} + e^{i[\frac{a_0}{4}(-q_x-q_y+q_z)]} + e^{i[\frac{a_0}{4}(q_x+q_y+q_z)]} - e^{i[\frac{a_0}{4}(-q_x+q_y-q_z)]} \right)$$

$$p_2 = -\left(-e^{i[\frac{a_0}{4}(q_x-q_y-q_z)]} - e^{i[\frac{a_0}{4}(-q_x-q_y+q_z)]} + e^{i[\frac{a_0}{4}(q_x+q_y+q_z)]} + e^{i[\frac{a_0}{4}(-q_x+q_y-q_z)]} \right)$$

$$p_3 = -\left(e^{i[\frac{a_0}{4}(q_x-q_y-q_z)]} - e^{i[\frac{a_0}{4}(-q_x-q_y+q_z)]} + e^{i[\frac{a_0}{4}(q_x+q_y+q_z)]} - e^{i[\frac{a_0}{4}(-q_x+q_y-q_z)]} \right)$$

$$q = -\left(e^{i[\frac{a_0}{4}(-q_x+q_y+q_z)]} + e^{i[\frac{a_0}{4}(q_x-q_y+q_z)]} + e^{i[\frac{a_0}{4}(-q_x-q_y-q_z)]} + e^{i[\frac{a_0}{4}(q_x+q_y-q_z)]} \right)$$

$$q_1 = -\left(-e^{i[\frac{a_0}{4}(-q_x+q_y+q_z)]} - e^{i[\frac{a_0}{4}(q_x-q_y+q_z)]} + e^{i[\frac{a_0}{4}(-q_x-q_y-q_z)]} + e^{i[\frac{a_0}{4}(q_x+q_y-q_z)]} \right)$$

$$q_2 = -\left(-e^{i[\frac{a_0}{4}(-q_x+q_y+q_z)]} + e^{i[\frac{a_0}{4}(q_x-q_y+q_z)]} + e^{i[\frac{a_0}{4}(-q_x-q_y-q_z)]} - e^{i[\frac{a_0}{4}(q_x+q_y-q_z)]} \right)$$

$$q_3 = -\left(e^{i[\frac{a_0}{4}(-q_x+q_y+q_z)]} - e^{i[\frac{a_0}{4}(q_x-q_y+q_z)]} + e^{i[\frac{a_0}{4}(-q_x-q_y-q_z)]} - e^{i[\frac{a_0}{4}(q_x+q_y-q_z)]} \right)$$

(20)

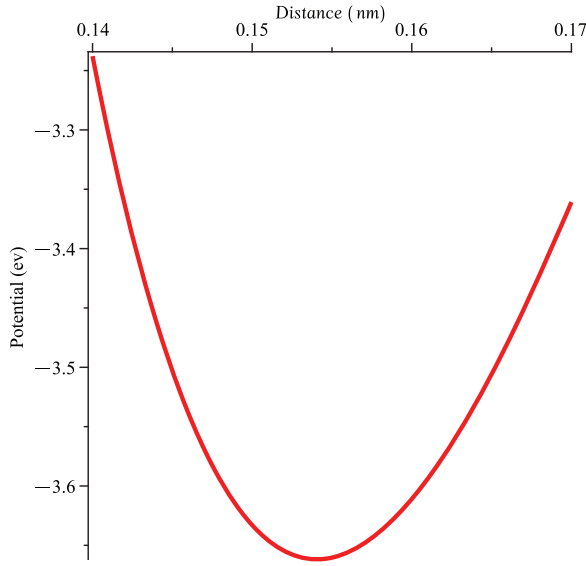where q_x, q_y, q_z are the components of $\mathbf{q}$.

Figure 3. Variation of original Brenner potential energy (per atom) with distance.

5. Parameter optimization

Variation of original Brenner potential's energy and its first-order derivative with distance are summarized in Figures 3 and 4.

The original Brenner potential can describe the tendency of cohesive energy for diamond. However, only a little experimental data, such as binding energy and lattice constant [27], can be used to determine the parameters, which cannot accurately determine the value of potential energy for different distances. Actually, the numerical results show that the variation tendency of original Brenner potential is slightly slow compared to the experimental data, so how to modify the Brenner potential is an important problem.

Since the thermodynamic properties, such as specific heat, CTE and Grüneisen parameters, can be predicted quite well based on the correct lattice constant one can now focus on the calculation of lattice constant. To calculate the lattice constant at different temperature, we should minimize the Helmholtz free energy A, instead of the potential energy U_{tot}, i.e.

$$\frac{\partial A(r, T)}{\partial r} = 0. \tag{21}$$

Since the Helmholtz free energy, A, takes the form [36,37]

$$A = U + k_B T \sum_j \ln\left[2 \sinh\left(\frac{\hbar \omega_j}{2 k_B T}\right)\right], \tag{22}$$

where k_B is the Boltzman constant $(1.38 \times 10^{-23} \, \text{J/K})$, $\hbar$ is the Planck's constant $(1.055 \times 10^{-34} \, \text{J s})$ and ω_j are the vibration frequencies of the system.
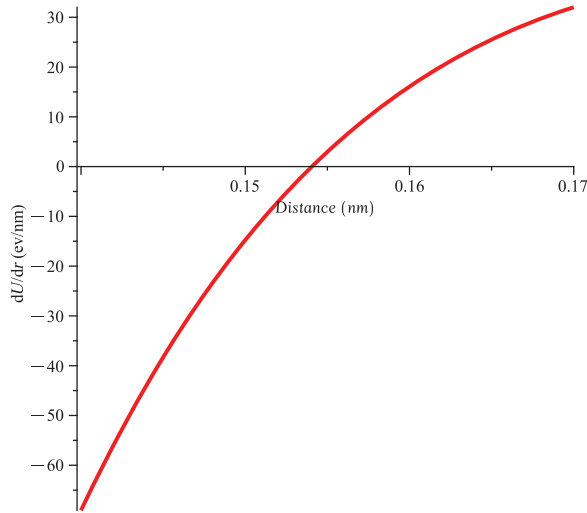
Figure 4. Variation of the first-order derivative of original Brenner potential energy (per atom) with distance.

Substituting Equation (22) into Equation (21), we have

$$\frac{\partial U}{\partial r} - T\frac{\partial S}{\partial r} = 0, \tag{23}$$

where $S = -k_B \sum_j \ln[2\sinh(\hbar\omega_j/2k_BT)]$. It is obvious that the equilibrium of potential force and entropy (TS) force ($-T\partial S/\partial r$) determines the lattice constant. The potential force, which tends to make the lattice constant equal to its original value, is opposite to the TS force. Thus, the ratio of the potential force $\partial U/\partial r$ to $T\partial S/\partial r$ determines the magnitude of the lattice constant. Furthermore, the numerous results show that the ratio of $\partial U/\partial r$ to $\partial^2 U/\partial r^2$ determines the shape of the CTE curve. Fortunately, the original Brenner potential gives the correct shape of the CTE curve, and we only need to keep this ratio.

However, there is another thing that needs to be considered. From Equations (19) and (20), one can clearly see that the squares of the vibration frequencies are approximately determined by a linear combination of the first-order and second-order derivative of the potential. Thus, in order to predict the accurate value of the specific heat, we should adjust the value of this linear combination.

Since the prediction on CTE given by original Brenner potential is remarkably higher than the experimental data, we change the parameter De in the original Brenner potential from 6.0 to 9.0. The optimized potential and its first-order derivative are shown in Figures 5 and 6. Since the value of binding energy at equilibrium distance should keep unchanged, we can add a constant, C, which equals to 1.83 eV:

$$V_{ij} = V_R(r_{ij}) - \bar{B}_{ij}V_A(r_{ij}) + C. \tag{24}$$

As discussed by Jiang et al. [13], with the original Brenner potential there is discrepancy between calculation and experiment for CTE, which is mainly because
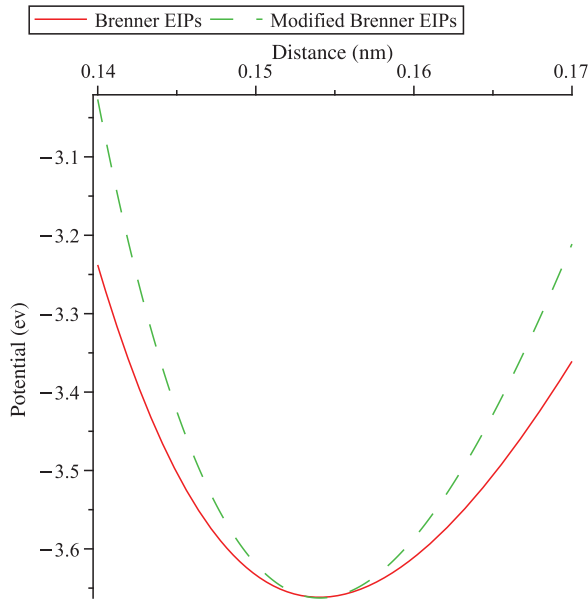
Figure 5. Variation of the original and optimized potential energy with distance.

the CTE is directly proportional to the derivative of vibration frequencies $d\omega/dr$. It is recalled from Equation (19) that ω^2 is determined by the first-order and second-order derivatives of the interatomic potential. Therefore, $d\omega/dr$ involves the third-order derivatives of the potential energy, which may not be accurate since the parameters in interatomic potentials are usually determined from the energy at the ground state, its first-order derivative (lattice constant) and second-order derivative (elastic moduli), but not third-order derivative [27,38]. Now, with the first-order derivative and second-order derivative of optimized Brenner potential, its third-order derivative is also changed, which enables calculation of CTE to predict the experimental data quite well.

It is worth noting that the value of the second-order derivative optimized Brenner potential is 1.5 times higher than the original one, which means the bulk modulus of the optimized Brenner potential approximately equals to 700 GPa. Since the bulk modulus of diamond and chemical vapor deposition (CVD) diamond is, respectively, 442 GPa [39] and 1200 GPa [40], 700 GPa for the optimized Brenner potential is acceptable.

6. Thermodynamic properties of diamond

All calculations in this paper are carried on for $10 \times 10 \times 10$, $1000 \times 100 \times 10$ and $100 \times 10 \times 100$ unit cells with periodic boundary conditions. It is shown that, with different numbers of unit cells being used, the results of thermodynamic properties are nearly identical. Thus, we just give one calculation curve instead of three in the following figures.
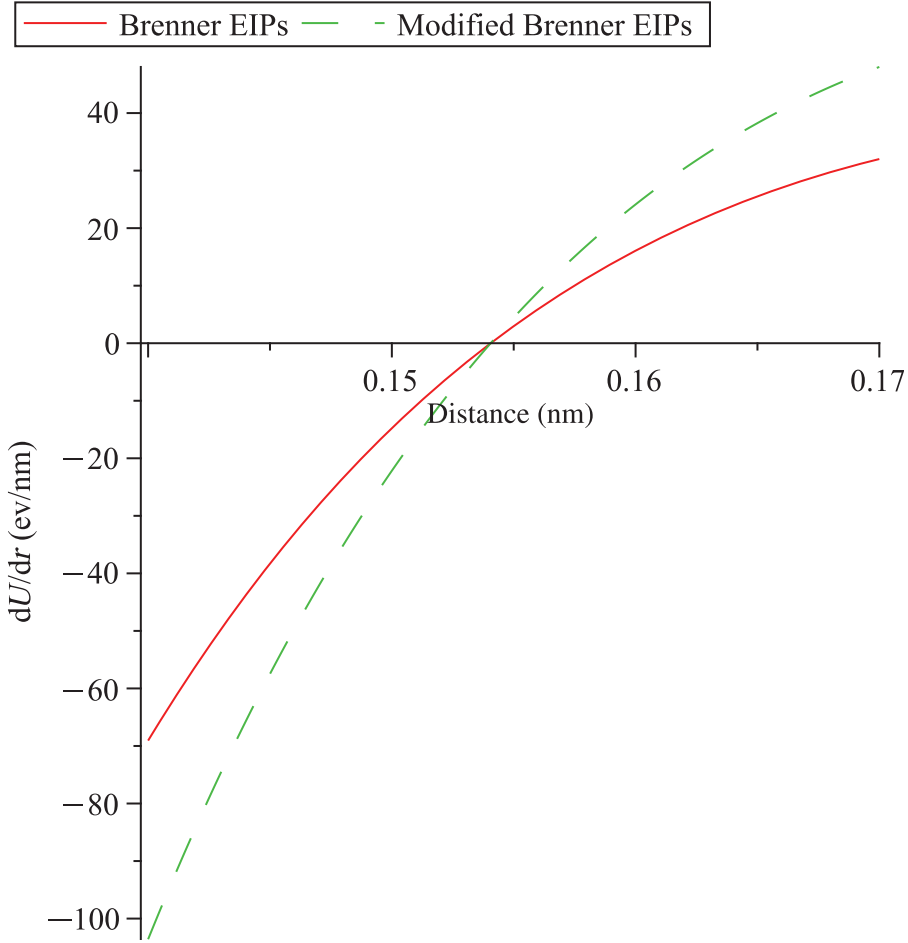
Figure 6. Variation of the original and optimized potential energy's first-order derivative with distance.

6.1. *The specific heat of diamond*

The total thermal energy and specific heat were given respectively by [41]

$$E(T) = \sum_{\mathbf{q}}^{N} \sum_{s=1}^{6} \left(\frac{1}{2} \hbar \omega_s(\mathbf{q}) + \frac{\hbar \omega_s(\mathbf{q})}{e^{\hbar \omega_s(\mathbf{q})/k_B T} - 1} \right)$$

$$C_V = \frac{\mathrm{d}E(T)}{\mathrm{d}T} = \sum_{\mathbf{q}}^{N} \sum_{s=1}^{6} \left(k_B \frac{(\hbar \omega_s(\mathbf{q})/k_B T)^2 e^{\hbar \omega_s(\mathbf{q})/k_B T}}{(e^{\hbar \omega_s(\mathbf{q})/k_B T} - 1)^2} \right) \tag{25}$$

where $\mathbf{q}$ takes N (N is the total primitive cell number) distinct values and $\omega_s(\mathbf{q}) = \sqrt{\lambda_s(\mathbf{q})/m}$, $(s = 1, 2, \ldots \ldots 6)$, is the frequency of the sth oscillator for a given $\mathbf{q}$.
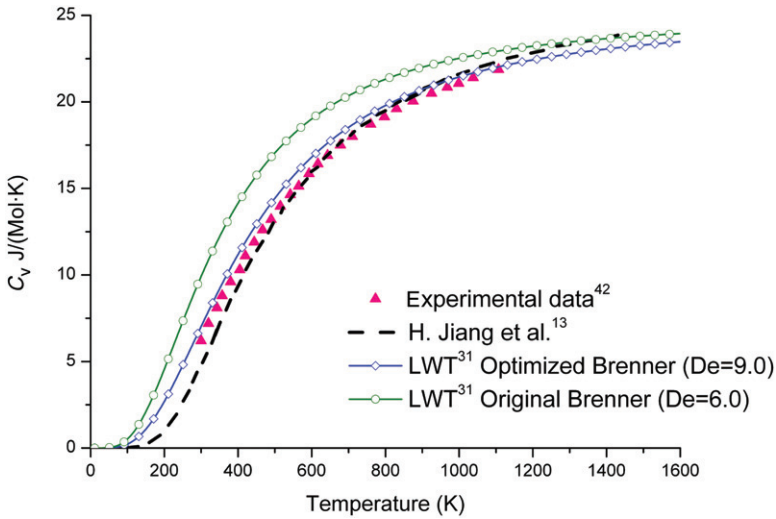
Figure 7. Temperature dependence of the specific heat, C_V, for diamond. The upper and lower solid lines are the calculation results of the lattice wave theory [31] (LWT) based on original and optimized Brenner potential, respectively; the experimental data [42] and the calculation result by Jiang et al. [13] with original Brenner potential are also shown for comparison.

In Figure 7, it can be seen that the result from the LWT [31] model with optimized Brenner potential is in good agreement with experimental data [42] over the entire range of temperature.

6.2. *Lattice constant*

We computed the zero pressure equilibrium distance $r_0(T)$ at various temperatures (0–2000 K) by using the optimized Brenner potential. The equilibrium distance $r_0(T)$ is obtained when the Helmholtz free energy A is minimized with respect to $r_0(T)$, i.e.

$$\frac{\partial A}{\partial r} = 0. \tag{26}$$

The result (Figure 8) obtained from the optimized Brenner potential agrees quite well with experimental data.

6.3. *CTE of diamond*

The coefficient of thermal expansion (CTE), α, is defined by

$$\alpha = \frac{1}{r_0(293\text{K})}\frac{\mathrm{d}r_0(T)}{\mathrm{d}T}, \tag{27}$$

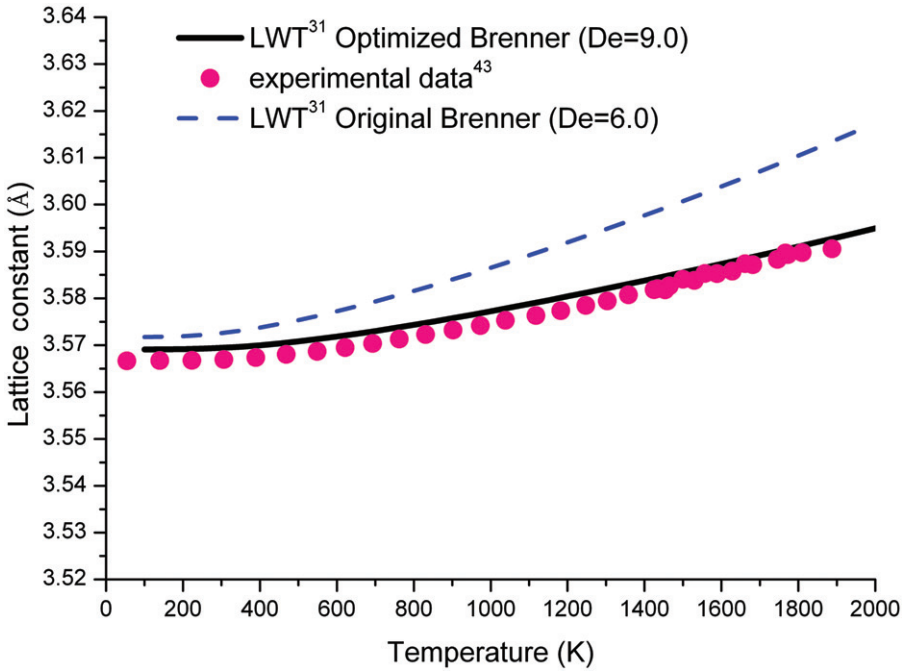where $r_0(T)$ is the bond length after thermal expansion at temperature T.

Figure 8. Variation of the lattice constant with temperature predicted by LWT [31] with original and optimized Brenner potential, and the experimental data [43].

As mentioned above, a correct lattice constant leads to an accurate prediction for CTE. Here the calculation result (in Figure 9) obtained from LWT theory with optimized Brenner potential predicts the CTE quite well over the entire range of temperature.

6.4. *Grüneisen parameters*

Since the specific heat and CTE are obtained, Grüneisen's rule can be used to calculate the Grüneisen parameters at different temperature, i.e.

$$\alpha = \frac{\gamma}{K_0}\frac{C_V}{V} \Rightarrow \gamma = K_0 V \frac{\alpha}{C_V}, \tag{28}$$

where K_0 is the bulk modulus, V is the volume, α is the CTE and C_V is the specific heat. The comparison between the computed Grüneisen parameters and the experimental data is shown in Figure 10.

With accurate prediction for both specific heat and CTE, one can expect that the calculation result of Grüneisen parameter is in good agreement with the experimental data.

7. Conclusion

In this paper, the lattice wave theory of molecular dynamics [31] (LWT) is used to calculate the thermodynamics properties of diamond, such as specific heat, CTE,
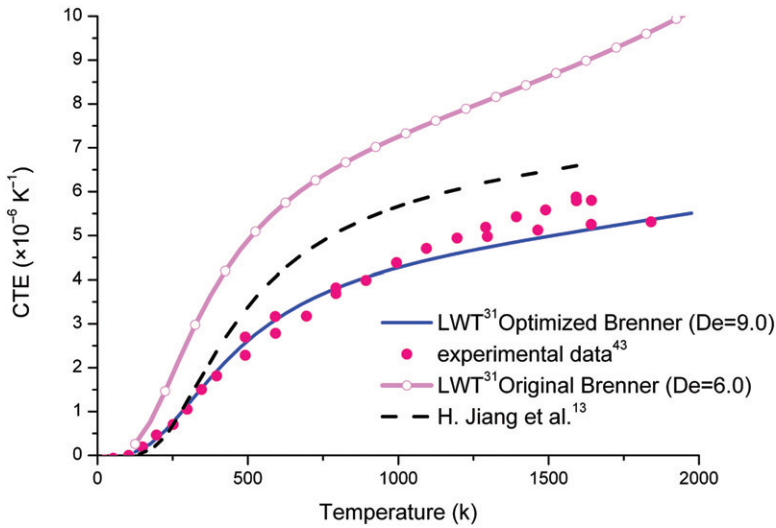
Figure 9. Variation of the CTE with temperature. The calculation results obtained from LWT [31] with original and optimized Brenner potential, the experimental data [43] and the calculation result by Jiang et al. [13] with original Brenner potential.
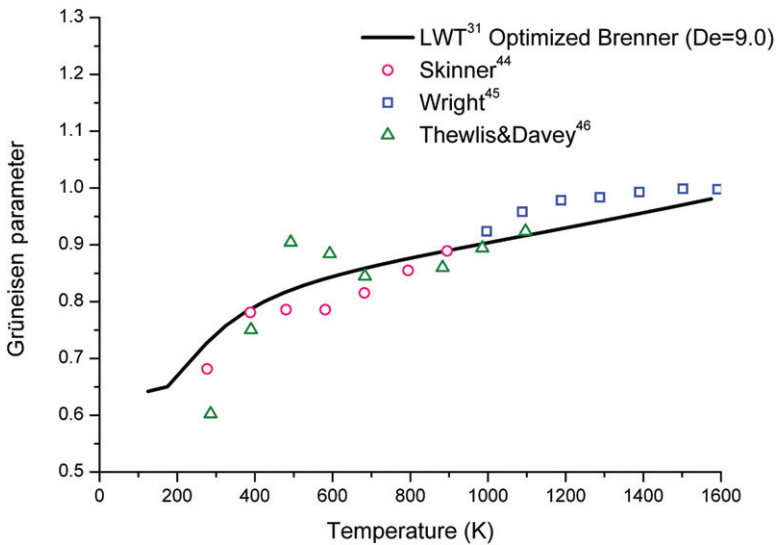

Figure 10. Variation of the Grüneisen parameters with temperature obtained from original and optimized Brenner potential (with LWT [31]), and the experimental data of Skinner [44], Wright [45] and Thewlis and Davey [46].

lattice constant and Grüneisen parameters. Since the variation tendency of the original Brenner potential is a slightly slow, a simple optimized Brenner potential is proposed and has been demonstrated to improve the prediction remarkably. The calculated thermodynamics properties of diamond have been found to be in very

good agreement with the corresponding measured values. This paper shows clearly that the simple optimized Brenner potential is suitable for diamond. But for other materials, it can be used only after systematic and careful testing. Meanwhile the present optimized Brenner potential can be used for the calculation of the mechanical properties, such as Young's modulus for diamond, when diamond is subjected to deformation. Thus, one can expect that the method to optimize parameters for Brenner potential may provide a reference for the calculation of thermodynamics properties based on other potentials in different systems.

Acknowledgments

References

[1] E.B. Tadmor, M. Ortiz and R. Phillips, Phil. Mag. A 73 (1996) p.1529.
[2] V.B. Shenoy, R. Miller, E.B. Tadmor, D. Rodney, R. Phillips and M. Ortiz, J. Mech. Phys. Solid 47 (1999) p.611.
[3] V. Shenoy, V. Shenoy and R. Phillips, Multiscale Model. Mater. 538 (1999) p.465.
[4] R.E. Miller and E.B. Tadmor, J. Comput.-Aided Mater. Des. 9 (2002) p.203.
[5] L.M. Dupuy, E.B. Tadmor, R.E. Miller and R. Phillips, Phys. Rev. Lett. 95 (2005) p.060202.
[6] M. Arroyo and T. Belytschko, J. Mech. Phys. Solid 50 (2002) p.1941.
[7] P. Zhang, Y. Huang, H. Gao and K.C. Hwang, J. Appl. Mech. 69 (2002) p.454.
[8] P. Zhang, Y.G. Huang, P.H. Geubelle and K.C. Hwang, Acta Mech. Sin. 18 (2002) p.528.
[9] P. Zhang, Y. Huang, P.H. Geubelle, P.A. Klein and K.C. Hwang, Int. J. Solid Struct. 39 (2002) p.3893.
[10] P. Zhang, H. Jiang, Y. Huang, P.H. Geubelle and K.C. Hwang, J. Mech. Phys. Solid 52 (2004) p.977.
[11] H. Jiang, P. Zhang, B. Liu, Y. Huang, P.H. Geubelle, H. Gao and K.C. Hwang, Comp. Mater. Sci. (Computational Materials Science) 28 (2003) p.429.
[12] J.H. Weiner, *Statistical Mechanics of Elasticity*, Wiley, New York, 1979.
[13] H. Jiang, Y. Huang and K.C. Hwang, J. Eng. Mater. 127 (2005) p.408.
[14] H. Zhao, Z. Tang, G. Li and N.R. Aluru, J. Appl. Phys. 99 (2006) p.064314.
[15] F. El-Mellouhi, W. Sekkal and A. Zaoui, Phys.: Stat. Mech. Appl. 311 (2002) p.130.
[16] J. Tersoff, Phys. Rev. B 37 (1988) p.6991.
[17] J. Tersoff, Phys. Rev. B 39 (1989) p.5566.
[18] W.L. Jorgensen, J.D. Madura and C.J. Swenson, J. Am. Chem. Soc. 106 (1984) p.6638.
[19] N.L. Allinger, K.S. Chen and J.H. Lii, J. Comput. Chem. 17 (1996) p.642.
[20] W.L. Jorgensen, D.S. Maxwell and J. TiradoRives, J. Am. Chem. Soc. 118 (1996) p.11225.
[21] W.D. Cornell, P. Cieplak, C.I. Bayly, I.R. Gould, K.M. Merz, D.M. Ferguson, D.C. Spellmeyer, T. Fox, J.W. Caldwell and P.A. Kollman, J. Am. Chem. Soc. 117 (1995) p.5179.
[22] T.A. Halgren, J. Comput. Chem. 17 (1996) p.490.
[23] S.K. Nath, F.A. Escobedo and J.J. de Pablo, J. Chem. Phys. 108 (1998) p.9905.
[24] M.G. Martin and J.I. Siepmann, J. Phys. Chem. B 102 (1998) p.2569.

[25] H. Sun, J. Phys. Chem. B 102 (1998) p.7338.
[26] S.J. Stuart, A.B. Tutein and J.A. Harrison, J. Chem. Phys. 112 (2000) p.6472.
[27] D.W. Brenner, Phys. Rev. B 42 (1990) p.9458.
[28] D.W. Brenner, Phys. Rev. B 46 (1992) p.1948.
[29] D.W. Brenner, J.A. Harrison, C.T. White and R.J. Colton, Thin Solid Film 206 (1991) p.220.
[30] A.V. Petukhov and A. Fasolino, Phys. Status Solidi (a) 181 (2000) p.109.
[31] Q.H. Tang and T.C. Wang, Science China G 41 (2011) p.214.
[32] Z. Tang, H. Zhao, G. Li and N.R. Aluru, Phys. Rev. B 74 (2006) p.64110.
[33] B.T.M. Willis and A.W. Pryor (eds.), *Thermal Vibrations in Crystallography*, Cambridge University Press, Cambridge, 1975.
[34] K. Huang and M. Born, *Dynamical Theory of Crystal Lattices*, Oxford University Press, New York, 1954.
[35] M. Born and T. von Karman, Phys. Z. 13 (1912) p.297.
[36] S.M. Foiles, Phys. Rev. B 49 (1994) p.14930.
[37] D. Chandler, *Introduction to Modern Statistical Mechanics*, Oxford University Press, Oxford, 1987, p.288.
[38] D.W. Brenner, O.A. Shenderova, J.A. Harrison, S.J. Stuart, B. Ni and S.B. Sinnott, J. Phys.: Condens. Matter 14 (2002) p.783.
[39] K. Huang and R. Y. Han, *Physics of Solid State* (in Chinese), Peking University Press, Beijing, 1982.
[40] P.W. May, Endeavour 19 (1995) p.101.
[41] N.W. Ashcroft and N. Mermin, *Solid State Physics*, Holt-Saunders, Tokyo, 1981.
[42] O. Madelung, M. Schulz, H. Weiss and Landolt-Börnstein (eds.), *Physics of Group IV Elements and III–V Compounds*, Springer-Verlag, Berlin, 1982.
[43] R.R. Reeber and K. Wang, J. Electron. Mater. 25 (1996) p.63.
[44] B.J. Skinner, Am. Mineral. 42 (1957) p.39.
[45] A.C.J. Wright, MSc Thesis, University of Reading, England, 1966 (Unpubulished).
[46] J. Thewlis and A.R. Davey, Phil. Mag. 1 (1956) p.409.